EUV Micro-Exposure Tool at 0.5 NA for Sub-16 nm Lithography

Michael Goldstein,[1,*] Russ Hudyma,[2] Patrick Naulleau,[3] and Stefan Wurm[1]

[1]SEMATECH, 255 Fuller Road, Albany, NY 12203, USA

[2]Hyperion Development, 358 South Overlook Drive, San Ramon, CA 94582, USA

[3]Center for X-ray Optics, Lawrence Berkeley National Laboratory, Berkeley, CA 94720, USA

[*]Corresponding author: michael.goldstein@sematech.org

The resolution limit of present 0.3 NA 13.5 nm wavelength micro-exposure tools is compared to next generation lithography research requirements. Findings suggest that a successor design is needed for patterning starting at the 16 nm semiconductor process technology node. A two-mirror 0.5 NA optical design is presented, and performance expectations are established from detailed optical and lithographic simulation. Here, we report on the results from a SEMATECH program to fabricate a projection optic with an ultimate resolution limit of approximately 11 nm.

OCIS codes: 110.0110, 110.4235, 220.0220, 220.3740, 340.0340, 340.7480.

Regular advances in lithography have been fundamental to the growth of the semiconductor industry.[1] However, it is becoming increasingly difficult to continue the exponential rate at which resolution has been scaling with optical (currently 193 nm wavelength) lithography. Progress in recent years has largely been achieved by a steady increase in exposure tool numerical aperture (NA) by wavefront engineering (with optical proximity correction, off-axis illumination, polarization, and phase mask imaging) and less frequently by reductions in exposure wavelength.[2,3,4] Although relatively expensive, double patterning techniques are likely to be adopted.[5] The anticipated evolution from optical to 13.5 nm wavelength extreme ultraviolet lithography (EUVL) represents the next significant transition for the semiconductor industry, necessitating the creation of new tools to support photoresist and mask research.[6]

The development of an EUV infrastructure has been complicated by a scarcity of high resolution research equipment. Figure 1(a) shows the optical design of the Berkeley EUV micro-exposure tool (MET1), one of two METs operated by SEMATECH.[7] As far as the authors know, only four EUV METs exist worldwide as of this writing.[8,9,10] Figure 1(b) shows simulated image contrast as a function of feature size and coherence for the MET1. The calculation used design aberrations (40 mλ RMS) at the 200×200 μm field corner with 7% flare. Recent scanning electron micrographs from the tool are shown in figure 1(c). Near diffraction limited imaging down to a half-period of approximately ~22 to 25 nm is possible; however, further progress below that resolution is limited by the projection optics. This is a concern as EUVL is expected to enter high volume manufacturing (HVM) at or below the 22 nm half-period node. Non-imaging EUV interference lithography (EUV-IL) tools have been developed at synchrotron facilities,[11,12,13] and interest in standalone tools is growing.[14,15,16,17] However, EUV-IL cannot support mask research, and the rate of progress for photoresist development continues to be equipment-limited.

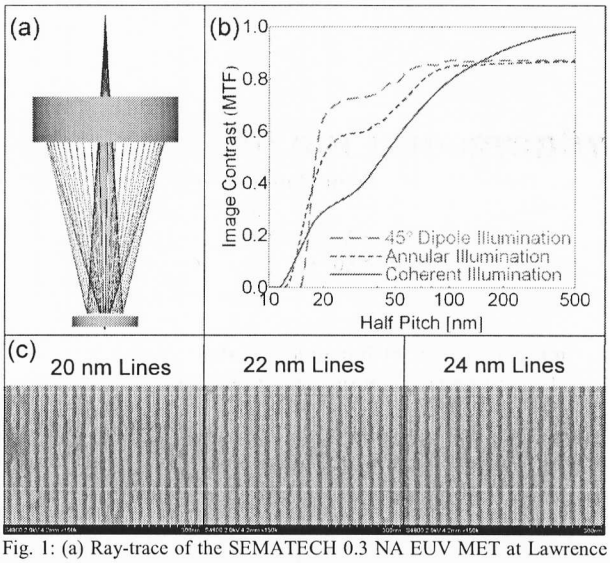

Fig. 1: (a) Ray-trace of the SEMATECH 0.3 NA EUV MET at Lawrence Berkeley National Laboratories Advance Light Source, (b) Image contrast versus resolution for coherent, 0.35/0.55 radii annular, and 0.1/0.57 radii 45° rotated dipole illumination, and (c) SEM images exposed at a dose of 15.2 mJ/cm^2 using the dipole illumination setting.

Three potential successors to the MET1 are shown in figure 2. All are 0.5 NA (MET2) designs constrained to the same track length of the existing MET1 system. A minimum working distance (≥5 mm) and maximum secondary mirror diameter (≤280 mm) were additional requirements to accommodate available focus sensors and platform mechanics. The 5× design in figure 2(a) uses near-equal radii mirrors. This minimizes the Petzval sum however increases the secondary diameter and reduces the spacing between it and the mask (object) plane, which constrains maximum partial incoherence. Slightly reducing the curvature ratio of the mirrors to 0.78 satisfied our packaging constraints and provided additional space for the illumination system. This 5× design, shown in figure 2(b), was selected to meet a majority of our requirements with a slightly reduced (~0.8×) field size. A four bounce two-mirror system was investigated to increase field size as

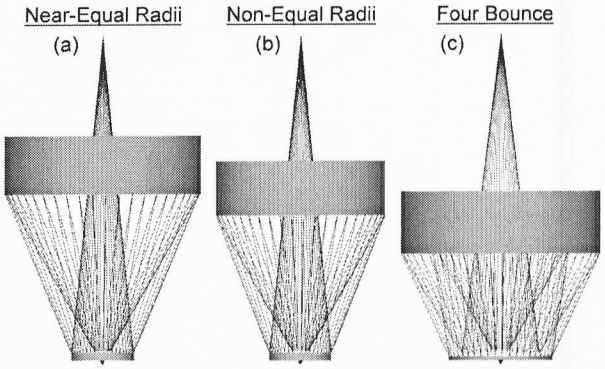

Fig. 2: Three 0.5 NA EUV (MET2) optical designs; (a) Near-equal radii with 5× demagnification, (b) Radii ratio of 78% with 5× demagnification, and (c) Four reflections with a 4× demagnification.

shown in figure 2(c). However, this increased the obscuration, decreased transmission, and exhibited middle frequency components in the wavefront. Additionally, it produced a very high aspect ratio primary and an unacceptably large secondary mirror.

Reflective EUVL photomasks used by EUVL are positioned at an oblique plane to separate illuminating and diffracted rays. We chose a chief ray angle of 6.0 degrees at the mask, which is the angle planned for first generation HVM equipment. A non-telecentric design introduces several complexities for HVM tools. However, the significant effect in the MET2 is a reduction of the field size. The usable field is chiefly limited by astigmatism for in-plane displacement and from spherical aberration for axial offsets. Figure 3(a) shows the calculated RMS wavefront error and phasemaps over a 30×200 μm field. The central obscuration, which is 7.1% of the pupil by area, is shown on the phasemaps. Lithographic performance is modeled at the edge-of-field analysis point, which has wafer (image) scale coordinates of {−100 μm, +15 μm}. Careful attention was given to optimizing performance over utilized areas of the pupil while minimizing the aspheric departure. The primary and secondary mirror surface departures from best RMS spherical fits are shown in figures 3 (b). The inner and outer semi-diameter of the primary mirror is 12.137956 and 45.544835 mm. The aspheric departure over this span has a maximum and range of 31 and 44 microns, respectively. The secondary mirror has an inner and outer semi-diameter of 23.175191 and 124.152614 mm with an aspheric departure and range of 39 and 56 microns.

Uniform reflective coatings were designed for the primary and secondary mirrors, encompassing incidence angles in the ranges of 0–5 and 7.5–12.5 degrees, respectively. The primary was optimized to minimize s-p polarization phase difference upon reflection. Retardance across the pupil and diattenuation (change in transmissions for s/p polarizations) were minimized to reduce horizontal/vertical feature size bias. Importantly, the design ensures that visible and EUV interferometric alignment are correlated. An axial astigmatism of ~6 milliwaves is present for linearly polarized input; however, this is averaged out with unpolarized illumination at the mask.

Equal line/space image contrast is shown for the analysis point with 7% flare in figure 4(a) for illumination that is coherent, 0.3/0.55 annular, and 0.1/0.57 radii dipole rotated at 45 degrees. A contour plot at best focus of a 16 nm equal line/space elbow pattern is shown in figure 4(b). The corresponding aerial image through focus and Bossung curves are shown in figure 4 (c) and (d), respectively. A 100 nm depth of focus is observed. Grouped/isolated line contrast exhibits an iso-coherence point at ~12 and ~27 nm, respectively, with annular illumination fixed at the central stop (σ_{inner} = 0.27) and an adjusted outer annulus (0.27 ≤ σ_{outer} ≤ 1.0). For smaller features, grouped line contrast improves with increasing partial incoherence (larger σ_{outer}) below the iso-coherence point at the expense of contrast for larger feature sizes. This relationship is reversed for isolated lines with smaller features showing increased contrast below the iso-coherence point for decreasing partial incoherence (smaller σ_{outer}). Annular illumination $\sigma_{inner}/\sigma_{outer}$ = 0.30/0.55 was selected for simultaneous 16 nm grouped and isolated line resolution. However, a system that is capable of adjustable partial coherence has benefits. Higher resolution is possible by optimizing isolated or grouped line patterning, each at the expense of the other. Simultaneous imaging down to 11 nm is possible with dipole illumination. Figure 4 (e) and (f) show the aerial image intensity through focus and Bossung curves for 11 nm equal line/space features using 45 degree rotated dipole illumination with a 0.1 pole radii and 0.57 pupil positions at the analysis point with 7% flare. Although not fully optimized, a depth of focus of 60 nm is obtained.

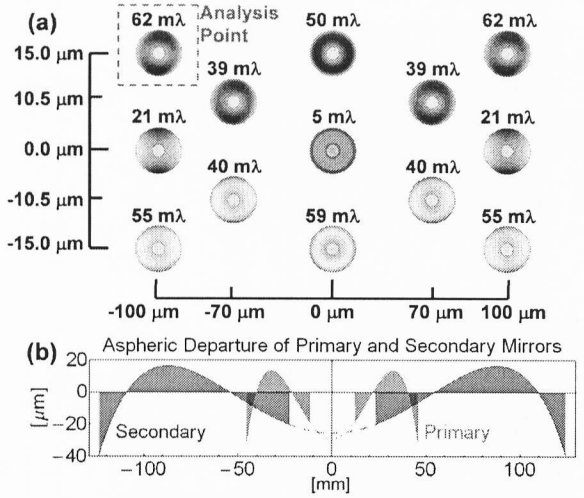

Fig. 3: (a) Aberration phasemaps and RMS wavefront errors over the 30×200 μm MET2 field. Piston, tilt, and defocus removed individually from the phasemaps and retained in RMS errors. The central obscuration is 7.1% of the pupil area, and the analysis point is outlined. (b) Primary and secondary mirror aspheric departures from RMS best fit spheres.

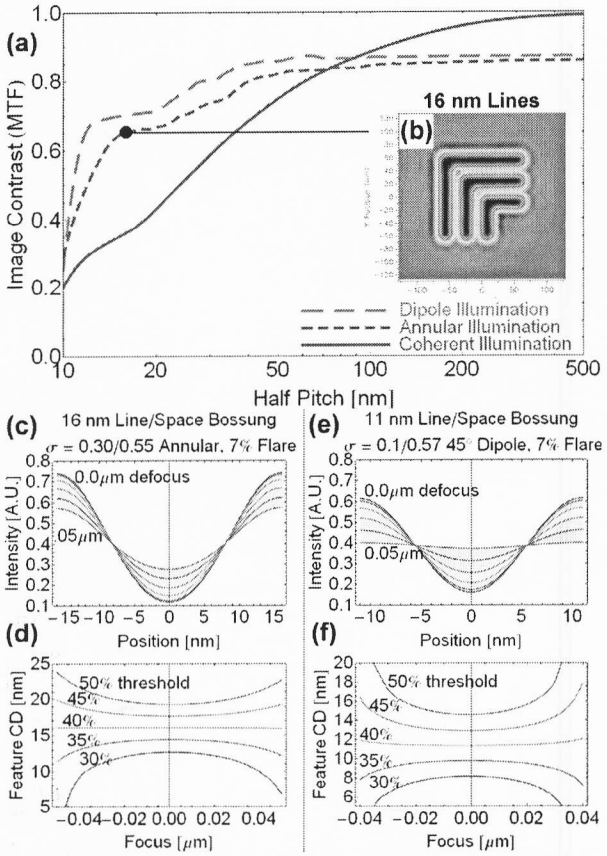

Fig. 4: (a) Equal line/space image contrast at the analysis point with 7% flare for coherent, 0.30/0.55 radii annular, and 0.1/0.57 radii 45° rotated dipole illumination. (b) Aerial image contours of 16 nm elbow feature, (c) 16 nm line/space aerial image intensity and (d) Bossung curves with annular illumination, (e) 11 nm line/space aerial image intensity and (f) Bossung curves with dipole illumination.

Our intention is to integrate the MET2 optic described above into a complete micro-field exposure tool at Lawrence Berkeley National Laboratory's Advanced Light Source synchrotron radiation facility (ALS). The new tool will be similar in design to the MET1.[7] High brightness/coherence is a significant benefit of synchrotron light sources. While coherence is typically a detriment in lithography, starting with high levels of coherence enables controlled and efficient generation of different partially coherent illumination settings using a source divergence synthesis process.[18] In conventional sources, etendue is often larger than that of the optical system and coherence control compromises optical efficiency. Another benefit of synchrotron sources is the lack of debris and spectral purity problems, thereby facilitating the design of the illumination optics. The crucial focus control capability will be provided by the same vacuum-compatible sub-nm height-sensor system developed for the MET1.[19]

METs are key enablers of EUV infrastructure progress, and early tool access is indispensable for timely photoresist and mask development, material evaluation, and defect printability studies. Supporting standard 150 mm masks and 300 mm wafers, the new tool will provide the first industry learning vehicle with high NA EUV optics. The MET2 will continue SEMATECH's EUVL program into future semiconductor process technology nodes.[20]

In summary, EUV lithography at a resolution of ~22 to 25 nm has been achieved and a 0.5 NA micro-exposure optic has been designed for extendibility. Benefit from adjustable partial coherence is expected and implementation is planned at the Berkeley ALS. Simulated performance results exceed our 16 nm needs, and an ultimate resolution of approximately 11 nm is possible.

1. G. Moore, "Cramming more components onto integrated circuits", Electronics **38**(8), 114 – 117 (1965).
2. T. Matsuyama, Y. Ohmura, D. M. Williamson, "The Lithographic Lens: its history and evolution," Proc. of SPIE **6154**, 1–14 (2006).
3. A. Wong, *Resolution Enhancement Techniques in Optical Lithography* (SPIE Press, 2001).
4. C. Spence, "Full-Chip Lithography Simulation and Design Analysis – How OPC is changing IC Design," Proc. of SPIE **5751**, 1–14 (2005).
5. M. Dusa, et. al., "Pitch Doubling Through Dual Patterning Lithography Challenges in Integration and Litho Budgets," Proc. of SPIE 6520, 1 – 10 (2007).
6. "International Technology Roadmap for Semiconductors," http://public.itrs.net.
7. P. Naulleau, J. Cain, E. Anderson, K. Dean, P. Denham, K. Goldberg, B. Hoef, K. Jackson, "Extreme ultraviolet lithography capabilities at the advanced light source using a 0.3-NA optic," IEEE J. Quantum Electron. **42**, 44-50 (2006).
8. J. Roberts, T. Bacuita, R. L. Bristol, H. Cao, M. Chandhok, S. H. Lee, M. Leeson, T. Liang, E. Panning, B. J. Rice, U. Shah, M. Shell, W. Yueh, G. Zhang, "Exposing extreme ultraviolet lithography at Intel," Microelectron. Eng. **83**(1 – 4), 672-675 (2006).
9. N. Nishimura, G. Takahashi, T. Tsuji, H. Morishima, K. Kajiyama, S. Uzawa, "Study of system performance in SFET," Proc. of SPIE **6921**, 1 – 9 (2008).
10. A. Brunton, *et al.*, "High-resolution EUV imaging tools for resist exposure and aerial image monitoring," Proc. SPIE **5751**, 78-89 (2005).
11. V. N. Golovkina, P. F. Nealey, F. Cerrina, J. W. Taylor, H. H. Solak, C. David, J. Gobrecht, J. Vac. Sci. Technol. B, **22**(1), 99 (2004).
12. Y. C. Cheng, A. Isoyan, J. Wallace, M. Khan, F. Cerrina, Appl. Phys. Lett. **90**, 023116, (2007).
13. A. Isoyan, A. Wüest, J. Wallace, F. Jiang, F. Cerrina, "4X reduction extreme ultraviolet interferometric lithography," Opt. Express **16**(12), 9106 – 9111 (2008).
14. M. Wei, D. Attwood, T. Gustafson, E. Anderson, J. Vac. Sci., Technol. B **12**, 3648 (1994).
15. M. Goldstein, D. Barnhart, R. D. Venables, B. V.D. Meer, Y. A. Shroff, Proceedings of the 2006 Int. Symposium on EUV Lithography, Barcelona. (2006).
16. P. Naulleau, C. Anderson, S. Horne, "Extreme ultraviolet interference lithography with incoherent light," Proc SPIE **6517**, 65172T (2007).
17. M. Goldstein, A. Wüest, D. Barnhart, "Partially-Coherent Extreme Ultraviolet Interference Lithography for 16 nm Patterning Research," Appl. Phys. Lett. **93**(8), 083110 1 – 3 (2008).
18. P. Naulleau, K. Goldberg, P. Batson, J. Bokor, P. Denham, and S. Rekawa, "A Fourier-synthesis custom-coherence illuminator for EUV microfield lithography," Appl. Opt. **42**, 820-826 (2003).
19. P. Naulleau, P. Denham, and S. Rekawa, "Design and implementation of a vacuum compatible laser-based subnanometer resolution absolute distance measurement system," Opt. Eng. **44**, 13605-13609 (2005).
20. S. Wurm C. Jeon, M. Lercel, "SEMATECH's EUV Program: A Key Enabler for EUVL Introduction," Proc. of SPIE 6517, 651705 (2007).